Planta (2020) 251:77
https://doi.org/10.1007/s00425-020-03355-9

ORIGINAL ARTICLE

A nucleoside diphosphate kinase gene *OsNDPK4* is involved in root development and defense responses in rice (*Oryza sativa* L.)

Jin Ye[1,2] · Wona Ding[1] · Yujie Chen[1] · Xinni Zhu[1] · Jiutong Sun[1] · Wenjuan Zheng[1] · Botao Zhang[3] · Shihua Zhu[1]

Received: 8 December 2019 / Accepted: 1 February 2020

Abstract

Main conclusion **Dysfunctional mutation of *OsNDPK4* resulted in severe defects in root development of rice. However, the resistance of *Osndpk4* against bacterial blight was significantly enhanced.**

Abstract Nucleoside diphosphate kinases (NDPKs) are an evolutionarily conserved family of important enzymes balancing the energy currency nucleoside triphosphates by catalyzing the transfer of their phosphate groups. The aim of this study was to elucidate the function of OsNDPK4 in rice. A dysfunctional rice mutant was employed to characterize the function of *OsNDPK4*. Its expression and subcellular localization were examined. The transcriptomic change in roots of *Osndpk4* was analyzed by RNA-seq. The rice mutant *Osndpk4* showed severe defects in root development from the early seedling stage. Further analysis revealed that meristematic activity and cell elongation were significantly inhibited in primary roots of *Osndpk4*, together with reduced accumulation of reactive oxygen species (ROS). Map-based cloning identified that the mutation occurred in the *OsNDPK4* gene. *OsNDPK4* was found to be expressed in a variety of tissues throughout the plant and OsNDPK4 was located in the cytosol. *Osndpk4* showed enhanced resistance to the bacterial pathogen *Xanthomonas oryzae* pv. *oryzae* (*Xoo*) and up-regulation of pathogenesis-related marker genes. In addition, transcriptomic analysis showed that *OsNDPK4* was significantly associated with a number of biological processes, including translation, protein modification, metabolism, biotic stress response, etc. Detailed analysis revealed that the dysfunction of *OsNDPK4* might reorchestrate energy homeostasis and hormone metabolism and signalling, resulting in repression of translation, DNA replication and cell cycle progression, and priming of biotic stress defense. Our results demonstrate that *OsNDPK4* plays important roles in energy homeostasis, development process, and defense responses in rice.

Keywords Defense responses · Nucleoside diphosphate kinases (NDPKs) · RNA-seq · Rice · Short root

Abbreviations

DEGs	Differentially expressed genes
GUS	β-Glucuronidase
KEGG	Kyoto Encyclopedia of Genes and Genomes
NDPK	Nucleoside diphosphate kinase
PR	Pathogenesis related
ROS	Reactive oxygen species
WT	Wild type
Xoo	*Xanthomonas oryzae* Pv. *oryzae*

Introduction

Nucleoside diphosphate kinases (NDPKs) are highly conserved enzymes ubiquitously found in various organisms from bacteria to human. They can catalyze the transfer of γ-phosphates from ATP to cognate nucleoside diphosphates

Communicated by Dorothea Bartels.

Jin Ye and Wona Ding contributed equally to this paper.

Electronic supplementary material The online version of this article (https://doi.org/10.1007/s00425-020-03355-9) contains supplementary material, which is available to authorized users.

✉ Wona Ding
dwn@zju.edu.cn

✉ Botao Zhang
zhangbotao@nimte.ac.cn

✉ Shihua Zhu
zhushihua@nbu.edu.cn

Extended author information available on the last page of the article

Published online: 09 March 2020

to sustain the balance between ATP and other nucleoside triphosphates (Parks and Aganwal 1973). NDPKs have been extensively studied in animal systems because of their potential application in the control of dissemination of tumor metastases, and they are found to play important roles in the regulation of cell proliferation, differentiation, invasion, and motility (Mehta and Orchard 2009).

The first plant NDPK was purified from pea seed in 1971 (Edlund 1971), and the first plant NDPK sequence was published 20 years afterwards (Nomura et al. 1992). With the help of recent advances in transcriptomic and proteomic approaches, it is now established that all plants contain a small NDPK gene family. Plant NDPKs have been less studied as compared with their animal counterparts. Nevertheless, they display a similar functional versatility in regulation of growth, development, and cellular metabolism. The *Arabidopsis ndpk2* mutant seedlings show poor germination, slow growth, and defects in cotyledon development (Choi et al. 2005; Verslues et al. 2007). Overexpression of the *PtNDPK2* gene in poplar resulted in significantly increased shoot heights, stem diameters, leaf number, and area compared with WT plants (Zhang et al. 2017). OsNDPK2 plays an important role in chlorophyll biosynthesis and chloroplast development, whose mutation results in significant change in major agronomic traits including plant height, seed-setting rate, flowering time, and tiller number (Ye et al. 2016). In *Solanum tuberosum*, NDPK1 is shown to regulate root growth, respiration, and carbon metabolism (Dorion et al. 2017). Furthermore, NDPK3a is involved in sugar metabolism in *Arabidopsis* (Hammargren et al. 2008).

Plant NDPKs also play important roles in tolerance to various abiotic stresses. AtNDPK1 was found to be involved in oxidative stress and interact with AtCAT1, 2, and 3 (Fukamatsu et al. 2003). Interaction between NDPK2 and catalase 1 (CAT1) was also reported in pea plants (Haque et al. 2010). Transgenic plants overexpressing *NDPK2* of *Arabidopsis*, poplar, and rice show enhanced multiple stress tolerance (Moon et al. 2003; Ye et al. 2016; Zhang et al. 2017). AtNDPK2 interacts with two mitogen-activated protein kinases, AtMPK3 and AtMPK6, to control cellular redox state (Moon et al. 2003). In addition, enhanced expression of *NDPKs* is found in response to wounding in tomato (Harris et al. 1994), salt treatment in rice and barley (Kawasaki et al. 2001; Fatehi et al. 2013), and glyphosate treatment in rice (Ahsan et al. 2008), suggesting a stress response mechanism linked to the expression of *NDPK* genes.

Plant NDPK isoforms were classified into four types (types I–IV) based on amino acid sequences (Dorion and Rivoal 2015). The rice genome contains five NDPKs, OsNDPK1–OsNDPK5. OsNDPK1 and OsNDPK4 are type I NDPKs, while OsNDPK2, OsNDPK3, and OsNDPK5 belong to type II, type III and type IV, respectively. Type I NDPKs have been reported to be the major (Cho et al. 2004) and the most active (Hetmann and Kowalczyk 2009). OsNDPK1 is the first studied NDPK in rice (Yano et al. 1993). The elongation of coleoptile cells was inhibited in *OsNDPK1* antisense transgenic plants (Pan et al. 2000). *OsNDPK1* was strongly induced by bacterial infection (Cho et al. 2004), drought stress (Salekdeh et al. 2002), salt stress (Kawasaki et al. 2001), and temperature stress (Lin et al. 2005; Lee et al. 2007; Chen et al. 2012). Moreover, the expression of *OsNDPK1* was highly induced after salicylic acid (SA), jasmonic acid, abscisic acid, and glyphosate treatment (Cho et al. 2004; Ahsan et al. 2008). A previous study showed that *OsNDPK4* was also induced by jasmonic acid (Cho et al. 2004). However, the function of OsNDPK4 during plant growth and development has not been characterized.

In this study, we isolate and characterize a new rice short root mutant *Osndpk4*. This mutant exhibits retarded root growth and defects in major agronomic traits. *OsNDPK4* is constitutively expressed in various tissues and developmental stages, and the protein is localized in the cytosol. OsNDPK4 also plays a role in disease resistance.

Materials and methods

Plant materials and growth conditions

The rice mutant *Osndpk4* was isolated from an ethylmethane sulfonate-mutagenized rice (*Oryza sativa* L. ssp.*indica*, cv Kasalath) mutant library (kindly provided by Prof. Ping Wu from Zhejiang University, China). Hydroponic experiments were conducted in rice culture solution with the pH adjusted to 5.5 (Zhu et al. 2012). After germination in water for 2 days in the dark, phenotypic characterization of the wild type (WT) and mutant was performed in a growth chamber at 30/22 ℃ (day/night) and 60–70% humidity with a photoperiod of 12 h. The WT and the mutant were grown in the paddy field under natural growing conditions for the evaluation of agronomic traits.

Histological observation

Histological sectioning examination was conducted as previously described (Ding et al. 2018). Briefly, root tips from 4-day-old plants were fixed overnight at 4 °C in 0.1 M sodium phosphate buffer (pH 7.2) with 2.5% glutaraldehyde, and washed three times for 30 min in the same buffer. Samples were then refixed in OsO_4 for 4 h at room temperature and washed for 30 min in the same buffer. Afterwards, samples were dehydrated in a gradient ethanol and embedded in pure Spurr resin and polymerized overnight at 70 °C. Semithin sections (2 µm thick) were made using diamond knives on a power Tome XL microtome (RMC-Boeckeler

Instruments, Tucson, AZ, USA) and stained with 0.1% methylene blue for 3–5 min at 70 °C. After rinsed with distilled water, images were taken with a microscope (Nikon 90i, Japan).

EdU staining

Primary root tips of 4-day-old WT and *Osndpk4* were stained with EdU using an EdU kit (C10350, Click-iT EdU Alexa Fluor 488 HCS assay; Invitrogen) according to the manufacturer's instruction. Roots were immersed in 20 mM EdU solution for 2 h before fixed for 30 min in 3.7% formaldehyde solution in phosphate buffer (pH 7.2) containing 0.1% Tritonx-100. Afterwards, they were incubated with EdU detection cocktail for 30 min and examined with a confocal laser-scanning microscope (Zeiss LSM 510, Jena, Germany). More than ten root samples of each genotype were examined.

Reactive oxygen species (ROS) and cell death detection

In situ H_2O_2 production was detected using an endogenous peroxidase-dependent staining procedure with 3,3-diaminobenzidine (DAB). Rice tissues were stained for 10 min in a solution of 1 mg/mL DAB in double-distilled water. Nitroblue tetrazolium chloride (NBT) staining was used for the detection of superoxide production (Carol et al. 2005). Rice tissues were stained for 10 min in a solution of 2 mM NBT in 20 mM phosphate buffer (pH 6.1). Cell death was examined using Evans Blue, a compound that selectively enters the dead cells (Gaff and Okong'O-Ogola 1971). Rice tissues were stained for 10 min in a solution of 1 mg/mL Evans Blue in double-distilled water before transferred to distilled water. Stained tissues were imaged using a microscope Nikon 90i. More than ten tissue samples were examined for each genotype, and the experiment was repeated twice.

Mapping and cloning of *OsNDPK4*

A mapping population was generated from crosses between the homozygous *Osndpk4* mutant and *japonica* variety Nipponbare. 30 and 1503 short root plants from the F_2 population were used for primary and fine mapping of *OsNDPK4*, respectively. The *OsNDPK4* gene was localized to a region of 114.7 kb between the sequence-tagged site markers In1 and In2 on chromosome 10. The *OsNDPK4* gene was selected out of 20 candidate protein-coding genes. Genomic DNA and mRNA regions of the *OsNDPK4* gene were amplified by PCR from both the WT and *Osndpk4* plants and analyzed by Sanger sequencing. Primers used were listed in Supplementary Table S1.

Construction of vectors and plant transformation

The coding region of *OsNDPK4* was PCR amplified and inserted into the pUCM-T vector (Takara). After confirmation by sequencing, the fragment was recovered from the pUCM-T vector by *Xba*I and *Kpn*I digestion and ligated into the corresponding site of pCAMBIA1300. A 2627 bp promoter of *OsNDPK4* was obtained by PCR and inserted into the *Hin*dIII/*Xba*I site in front of the *OsNDPK4* coding region to drive its expression. The promoter was also put into the *Hin*dIII/*Xba*I site of vector pCAMBIA1300NH-GUS to create a transcriptional fusion of the *OsNDPK4* promoter and the β-glucuronidase (GUS) coding sequence, *OsNDPK4p::GUS*. Above constructs were used for *Agrobacterium tumefaciens*-mediated rice transformation of WT or *Osndpk4* as described (Chen et al. 2003). Primers used are listed in Supplemental Table S1.

Histochemical analysis and GUS assay

Histochemical GUS staining was conducted as previously described (Ding et al. 2015). Plant samples and freehand cross-section samples were incubated with GUS staining solution (100 mmol/L NaH_2PO_4 buffer pH 7.0, 0.5% Triton X-100, 0.5 mg/mL X-Gluc and 20% methanol) overnight at 37 °C. Afterwards, tissues were rinsed and mounted on slides and photographed using a stereo microscope (Leica MZ95, Nussloch, Germany). More than five tissue samples were examined for each genotype or tissue type, and the experiment was repeated twice.

Subcellular localization of *OsNDPK4*

The full-length coding sequence of *OsNDPK4* without the stop codon was cloned and inserted in front of the coding sequence of a soluble modified green fluorescent protein (smGFP) in the modified pCAMBIA1300-35S-GFP vector using *Kpn*I and *Bam*HI. The resulting construct was sequenced to verify in-frame fusion and used for transient transformation of rice protoplasts (Miao and Jiang 2007). The pBWA(V)HS-mKATE empty vector was co-transformed as a cytosolic marker. The GFP and RFP were visualized using a confocal laser-scanning microscope Zeiss LSM 510. The experiment was repeated twice. Primers used are listed in Supplemental Table S1.

Determination of resistance to bacterial blight in *Osndpk4*

The bacterial blight resistance of *Osndpk4* was evaluated using three races of *Xoo*, the Philippines races PXO71, PXO99, and PXO145 kindly provided by Dr Jie Zhou of the Institute of Virology and Biotechnology, Zhejiang Academy

of Agricultural Sciences, China. New fully-expanded leaves of ten independent WT and *Osndpk4* plants at the maximum tillering stage were inoculated using the clipping leaf method (Kauffman et al. 1973). The lesion length on inoculated plants was measured 3 weeks after inoculation.

Quantitative real-time PCR analysis

RNA was extracted from leaves of WT and *Osndpk4* at the tillering stage using RNAiso plus (Takara). Three biological replicates of each genotype were collected to compare the expression in equivalent tissues in the WT and *Osndpk4* with the same genetic background. The first-strand cDNA was then synthesized using Superscript II (Invitrogen, Carlsbad, CA, USA) and used as templates. Real-time PCR analysis was conducted using an ABI 7500 System (Applied Biosystems Life Technologies) and UltraSYBR mixture with ROX (CWBio, Co., Ltd., Beijing, China). Primers used were listed in Supplementary Table S1. The *Ubiquitin* gene (*LOC_Os03g13170*) in rice was used as a reference gene.

Transcriptome sequencing

Total RNA was extracted from roots of 7-day-old WT and *Osndpk4* under normal condition using the RNeasy Plant Mini Kit (Qiagen). For each genotype, three biological replicates were collected to compare the expression in equivalent tissues in the WT and *Osndpk4* with the same genetic background. RNA samples were examined using the Nanodrop 2000 spectrophotometer (Thermo Fisher Scientific) and 2100 Bioanalyzer (Agilent Technologies). High-quality RNA samples for library construction were selected based on 260 nm/280 nm ratio and RNA integrity number above 2.0 and 7.0, respectively. Sequencing libraries were prepared using the TruSeq Stranded mRNA LTSample Prep Kit (Illumina) according to the manufacturer's instructions. Libraries were subjected to 125 cycles of paired-end sequencing with the Illumina HiSeq2500 system according to the manufacturer's instructions.

Differentially expressed gene analysis

Raw reads were first processed using NGS QC toolkit (v2.3.3). In this step, clean reads were obtained by removing reads containing adapter, reads containing ploy-*N*, and low-quality reads (the number of bases with quality value ≤ 20 is more than 35). The retained high-quality reads, i.e. clean reads, were then analysed by the TopHat-Cufflinks pipline (Trapnell et al. 2012). Briefly, clean reads were mapped to the rice genome (MSU version 7, https://rice.plantbiology.msu.edu/) using TopHat. Cufflinks was then used for transcriptome assembly and assessment of the FPKM value. Counts of mapped reads to genes were obtained with HTSeq (https://www-huber.embl.de/users/anders/HTSeq/doc/overview.html) and differentially expressed genes (DEGs) were determined using DESeq (https://bioconductor.org/packages/release/bioc/html/DESeq2.html) by the negative binomial distribution test based on the mapped reads of *Osndpk4* and WT (Love et al. 2014; Anders et al. 2015). Genes with an FDR-adjusted P value < 0.05 and fold change > 1.5 were assigned as DEGs. Gene ontology (GO) annotation was conducted by querying Swiss-prot (https://www.uniprot.org) with transcripts of DEGs and enrichment analysis was performed by the hypergeometric distribution test using R with a threshold FDR-adjusted P value < 0.01. The Kyoto Encyclopedia of Genes and Genomes (KEGG) pathway enrichment analysis was conducted by querying the KEGG database (www.kegg.jp) with a threshold FDR-adjusted P value < 0.05. The function categorization of DEGs was conducted by MapMan (Thimm et al. 2004). The clean reads data have been uploaded to the SRA (Sequence Read Archive, www.ncbi.nlm.nih.gov/sra) database (SRA accession: PRJNA518165).

Results

Rice *Osndpk4* is a mutant with short root and shoot

A short root mutant was isolated from an ethylmethane sulfonate-mutagenized rice mutant library (*Oryza sativa* L. *indica* cv. Kasalath). The mutant was designated *Osndpk4* based on our subsequent characterization of the mutant gene. During the early seedling stage, *Osndpk4* exhibited retarded root and shoot growth. The development of primary roots, adventitious roots, lateral roots, and root hairs in *Osndpk4* was significantly compromised compared with WT plants (Fig. 1a, b). *Osndpk4* also showed a less severe short shoot phenotype compared with the WT (Fig. 1a). Time-course analysis revealed that the short root and shoot phenotype of *Osndpk4* tended to become more severe along with growth time (Fig. 1c). Further analysis of relative growth rate confirmed that the relative growth per week of primary roots, adventitious roots, and shoots in *Osndpk4* was all lower than of WT during the first 5 weeks except the growth of shoots in the second week (Fig. 1d). To determine whether the short root phenotype of *Osndpk4* was due to defects in root cell elongation or division, root longitudinal section analysis for the WT and *Osndpk4* was first conducted. It revealed that cell length in elongation and maturation zones of the *Osndpk4* primary root was drastically reduced compared with the WT (Fig. 2a, b), suggesting inhibited cell elongation in root tips of *Osndpk4*. However, the root radical pattern organization and meristem of the mutant was not obviously different compared to the WT (Fig. 1d). Then a mitotic activity reporter, the *OsCYCB1,1:GUS*, was used

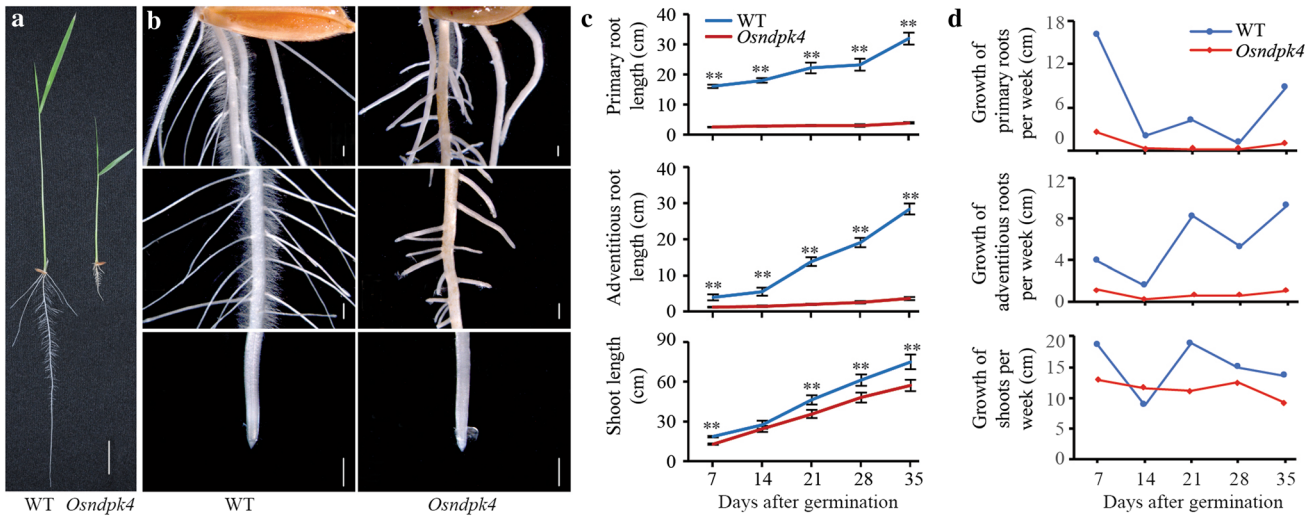

Fig. 1 Phenotypic characterization of *Osndpk4*. **a** Growth phenotype of 7-day-old WT and *Osndpk4*. Bar = 2 cm. **b** Stereomicroscope images of roots of the WT and *Osndpk4*. Bars = 500 µm. **c** Time course of the length of the primary root, adventitious root and shoot within the WT, and *Osndpk4* seedlings after germination. Error bars represent SD ($n = 10$). The asterisks in **c** indicate significant difference between WT and *Osndpk4* (**$P < 0.01$, by Student's t test). **d** Relative growth per week of primary roots, adventitious roots and shoots within WT, and *Osndpk4* seedlings after germination

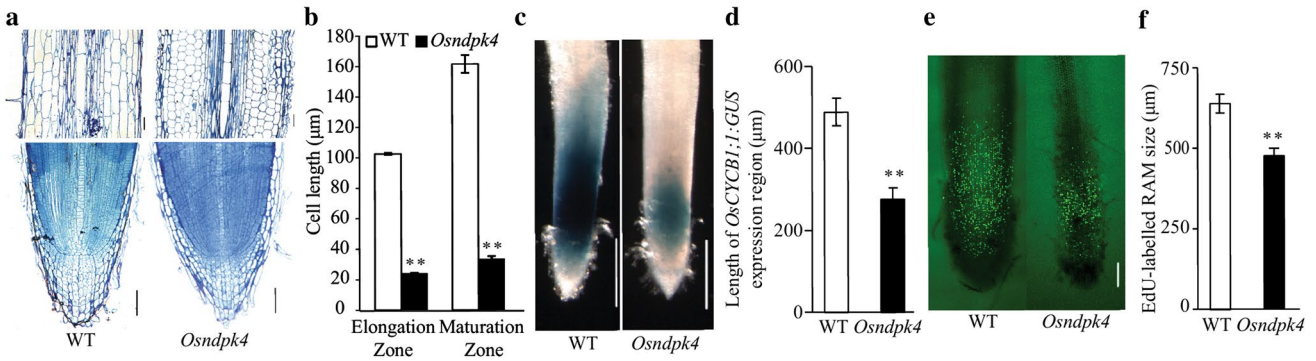

Fig. 2 Cell elongation and division activity in root tips of *Osndpk4*. **a** Longitudinal sections of the maturation zone (top) and root tip (bottom) of 3-day-old WT and *Osndpk4*. Bars = 50 µm. **b** Cell length in roots of 3-day-old WT and *Osndpk4*. Error bars represent SD ($n = 10$). **c** *OsCYCB1,1* promoter-GUS activity in primary root tips of 3-day-old WT and *Osndpk4*. Bars = 250 µm. **d** The length of stained regions in primary root tips of 3-day-old WT and *Osndpk4* in **c**. Error bars represent SD ($n = 10$). **e** S-phase entry of 4-day-old WT and *Osndpk4* root tips visualized by EdU staining. Bar = 100 µm. **f** Size of EdU-labelled root apical meristems of 4-day-old WT and *Osndpk4* in **e**. Error bars represent SD ($n = 10$). The asterisks in **b**, **d**, and **e** indicate significant difference between WT and *Osndpk4* (**$P < 0.01$, by Student's t test)

to examine whether the root mitotic activity in *Osndpk4* was affected. It was found that the expressing region of *OsCYCB1,1:GUS* in the primary root tip of *Osndpk4* was significantly shorter than that of the WT (Fig. 2c, d), indicating reduced cell division activity in root meristems of *Osndpk4*. To further determine the root meristem activity of *Osndpk4*, in situ incorporation of EdU, the thymidine analogue, into DNA during active DNA synthesis was visualized in the root tips of 4-day-old WT and *Osndpk4* seedlings (Ding et al. 2018). Consistent with the GUS staining, *Osndpk4* had significantly reduced levels of EdU labelling in the root meristem compared to the WT (Fig. 2e, f). Taken together, these results suggested that the shorter phenotype of the *Osndpk4* mutant was due to reduced cell elongation and division.

The mature-stage development of *Osndpk4* was also severely impaired (Fig. 3a–c). The plant height, panicle number, filled grain number per panicle, and root length of *Osndpk4* all significantly decreased compared with WT (Fig. 3d). However, there was no significant difference in the seed-setting rate between *Osndpk4* and WT (data not shown).

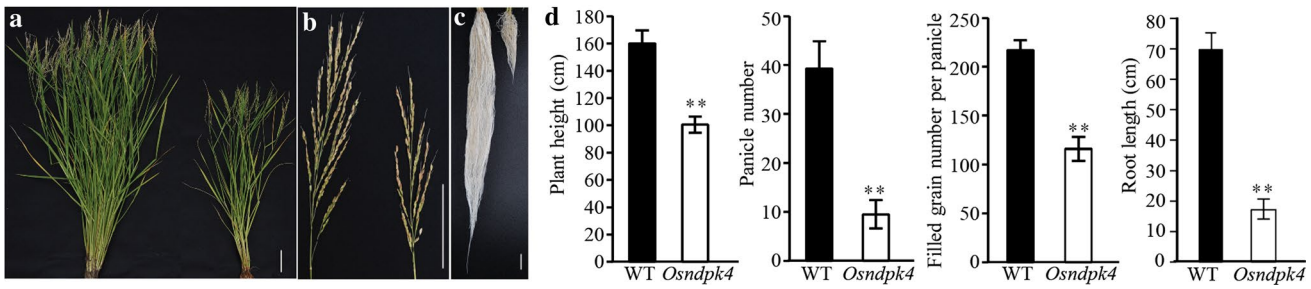

Fig. 3 Comparison of agronomic traits in WT and *Osndpk4*. **a** Aboveground parts of mature WT (left) and *Osndpk4* (right) plants from field planting. Bar = 10 cm. **b** Spikes of WT (left) and *Osndpk4* (right) from field planting. Bar = 10 cm. **c** Roots of WT (left) and *Osndpk4* (right) at the maturation stage from hydroponic culture. Bar = 4 cm. **d** Plant height, panicle number, filled grain number per panicle and root length of WT and *Osndpk4* at the maturation stage. Error bars represent SD ($n = 20$). The asterisks in **d** indicate significant difference between WT and *Osndpk4* (**$P < 0.01$, by Student's *t* test)

Enhanced cell death and reduction in ROS accumulation were observed in the root of *Osndpk4*

It was observed that roots of *Osndpk4* were more fragile than those of the WT. Staining of 7-day-old seedling roots with Evans blue (Gaff and Okong'O-Ogola 1971) demonstrated large stained patches near the root tips of *Osndpk4* mutant plants (Fig. 4a), indicating that cell death had occurred.

To investigate whether ROS levels were also altered in *Osndpk4*, we examined ROS levels in root tips of 7-day-old seedlings. In situ detection of O_2^- was performed using nitroblue tetrazolium chloride (NBT) staining (Carol et al. 2005), and H_2O_2 was analyzed using 3,3-diaminobenzidine (DAB) staining (Veljovic-Jovanovic et al. 2002). The results showed that *Osndpk4* accumulated significantly less O_2^- and H_2O_2 in the root tip compared to the WT (Fig. 4b, c), indicating that OsNDPK4 was critical for maintaining ROS levels in the root tip. However, no ROS accumulation was found in leaves of 7-day-old WT and *Osndpk4* (Supplementary Fig. S1).

Cloning of the *OsNDPK4* gene

To map the mutation in *Osndpk4*, a F_2 population was generated from a cross between *Osndpk4* and Nipponbare (*japonica*). The segregation of short root phenotype in the population showed a ratio of 3:1, with 168 plants of WT phenotype and 60 plants of *Osndpk4* phenotype ($\chi^2 = 0.21$, $P < 0.05$), suggesting that a single recessive gene was responsible for the mutant phenotype. Using 1503 mutant seedlings from the F_2 population, the mutation was mapped to a 114.7 kb region between InDel markers In1 and In2 on chromosome 10. This region contains 20 putative open reading frames (https://rice.plantbiology.msu.edu/), including a nucleoside diphosphate kinase 4 (*OsNDPK4*, LOC_Os10g41410) (Fig. 5a). Nucleoside diphosphate kinase was previously reported to be involved in regulation of cell division and growth in potato (Dorion et al. 2006), suggesting that *OsNDPK4* might be the possible candidate of the mutated gene. Therefore, the coding region of *OsNDPK4* in both the WT and *Osndpk4* was examined by Sanger sequencing. A point mutation (from C to T) was found in *Osndpk4* at the nucleotide position 706 bp of the gene region (from the initiation codon ATG) within the third exon of *OsNDPK4*, resulting in an

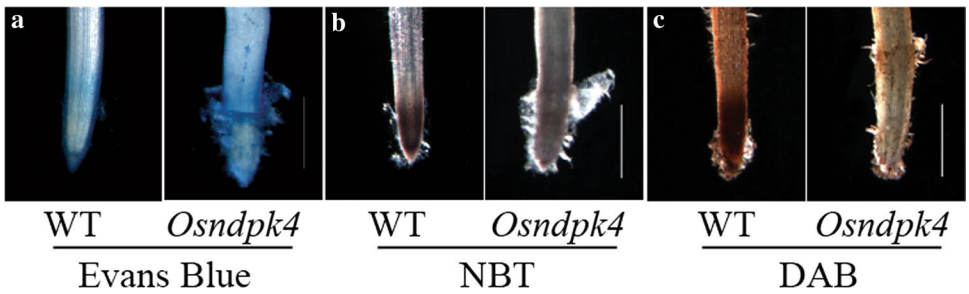

Fig. 4 ROS accumulation in root tips of WT and *Osndpk4*. **a** Evans blue staining for root cell death in primary root tips of the WT and *Osndpk4*. **b** Nitroblue tetrazolium chloride (NBT) staining for superoxide in primary root tips of the WT and *Osndpk4*. **c** 3,3-Diaminobenzidine (DAB) staining for hydrogen peroxide in primary root tips of the WT and *Osndpk4*. Bars = 500 μm

amino acid change (Ala^{108} to Val^{108}). The *OsNDPK4* gene was 2526 bp in length, and contained four exons and three introns. The protein-coding region of *OsNDPK4* was 456 bp and encodes a 151 amino acid protein. The annotation generated by the SMART database (https://smart.embl-heidelberg.de/) showed that it contained a conserved NDP domain (Fig. 5b, c). Alignment analysis of NDPK proteins showed that the mutated Ala^{108} residue was highly conserved among rice and *Arabidopsis* (Fig. 5d), which is consistent with the severe phenotype of *Osndpk4*.

Genetic complementation analysis was conducted to confirm whether the point mutation in *Osndpk4* was responsible for the mutant phenotype. The protein-coding region of *OsNDPK4* was cloned into a binary vector pCAMBIA1300 driven by its 2627 bp native promoter and used for transformation of *Osndpk4*. More than ten independent transgenic lines were obtained. The short root and shoot phenotype was restored in all the positive transformants (Fig. 5e), indicating that the mutant phenotype was caused by the point mutation in *OsNDPK4*.

Expression pattern and subcellular localization analysis of OsNDPK4

To examine the tissue expression pattern of *OsNDPK4*, a native promoter (2627 bp before the ATG) was fused to the GUS reporter gene. This chimeric gene cassette was used to transform Kasalath via the *Agrobacterium tumefaciens*-mediated transformation method. The GUS protein was observed ubiquitously in the rice plants included in root, leaf, pistils, stamen, glume, and stem node. Strong expression was observed in root tips and lateral root tips of primary roots and adventitious roots (Fig. 6a–i).

To examine the subcellular localization of OsNDPK4, a chimeric fusion gene of coding region of *OsNDPK4* and GFP under the control of the 35S promoter was constructed and transient expressed in rice protoplasts. Confocal microscopy revealed that the OsNDPK4-GFP signals co-localized with the red fluorescence signal of pBWA(V)HS-mKATE, a cytosolic marker, indicating that OsNDPK4 was localized in the cytosol (Fig. 6j).

Enhanced disease resistance in *Osndpk4*

Phylogenetic analysis indicated that there are four types of NDPK family genes in rice, and *OsNDPK4* and *OsNDPK1* belong to type I (Dorion and Rivoal 2015). OsNDPK1 was previously reported to be involved in defense response of rice against bacterial infection (Cho et al. 2004). To examine whether *Osndpk4* also gains disease resistance, WT and *Osndpk4* plants were inoculated with three races of *Xoo*, the causal agent of rice bacterial blight. The *Osndpk4* plants exhibited significantly enhanced resistance to all tested *Xoo* strains (PXO71, PXO99, and PXO145) compared to WT (Fig. 7a, b).

To analyze whether the expression of defense-related genes was up-regulated in *Osndpk4*, we performed qRT-PCR using selected defense-related genes. We examined gene expression patterns of two representative defense-related genes: pathogen-related (PR) protein 1a *PR1a* (LOC_Os07g03710) and peroxidase *PO-C1* (LOC_Os07g48050), which have been reported as up-regulated genes after pathogen attack or treatment with a plant-defense activator (Kano et al. 2010; Feng et al. 2013). The result showed that the tested defense-related genes *PR1a* and *PO-C1* were highly up-regulated in *Osndpk4* (Fig. 7c).

Whole-genome expression analysis of *Osndpk4*

To further gain insight into the *in planta* function of *OsNDPK4*, transcriptome sequencing analysis of WT and *Osndpk4* was conducted using RNA-seq. One-week-old root samples were selected for the profiling analysis and three replicates of each genotype were used. A total of 10,263 differentially expressed genes (DEGs) were identified with a cut-off of FDR-adjusted P value < 0.05 and fold change > 1.5. Among them, 5303 DEGs showed higher expression in *Osndpk4* than the WT and were termed as up-regulated genes, while 4960 DEGs showed lower expression in *Osndpk4* than the WT and were termed as down-regulated genes (Supplementary Table S2).

To analyze the general effect of *OsNDPK4* mutation on transcriptomes, gene ontology (GO) classification analysis of the up- and down-regulated DEGs was conducted (Fig. 8a, b, Supplementary Table S3). Within the category of biological process, up-regulated genes were largely associated with protein modification process, response to stress, metabolic process and cell death, indicating that the metabolic reprogramming and stress response was activated in *Osndpk4*. Genes involved in translation, photosynthesis, metabolites and energy, cellular component organization, DNA metabolism, and cell cycle were significantly enriched among down-regulated genes, indicating the general suppression of cell division and proliferation, which was consistent with the observed severe defects of root development in *Osndpk4*. Among the category of molecular function, genes involved in kinase activity and catalytic activity and a number of binding activity were the most enriched among up-regulated genes, while only genes involved in structural molecular activity, molecular function, and RNA binding were significantly enriched among down-regulated genes. In terms of cellular component, plasma membrane, vacuole, and peroxisome were significantly enriched among up-regulated genes, while down-regulated genes showed association with ribosome, plastid, membrane, nucleolus, mitochondrion, cytosol, and cell wall.

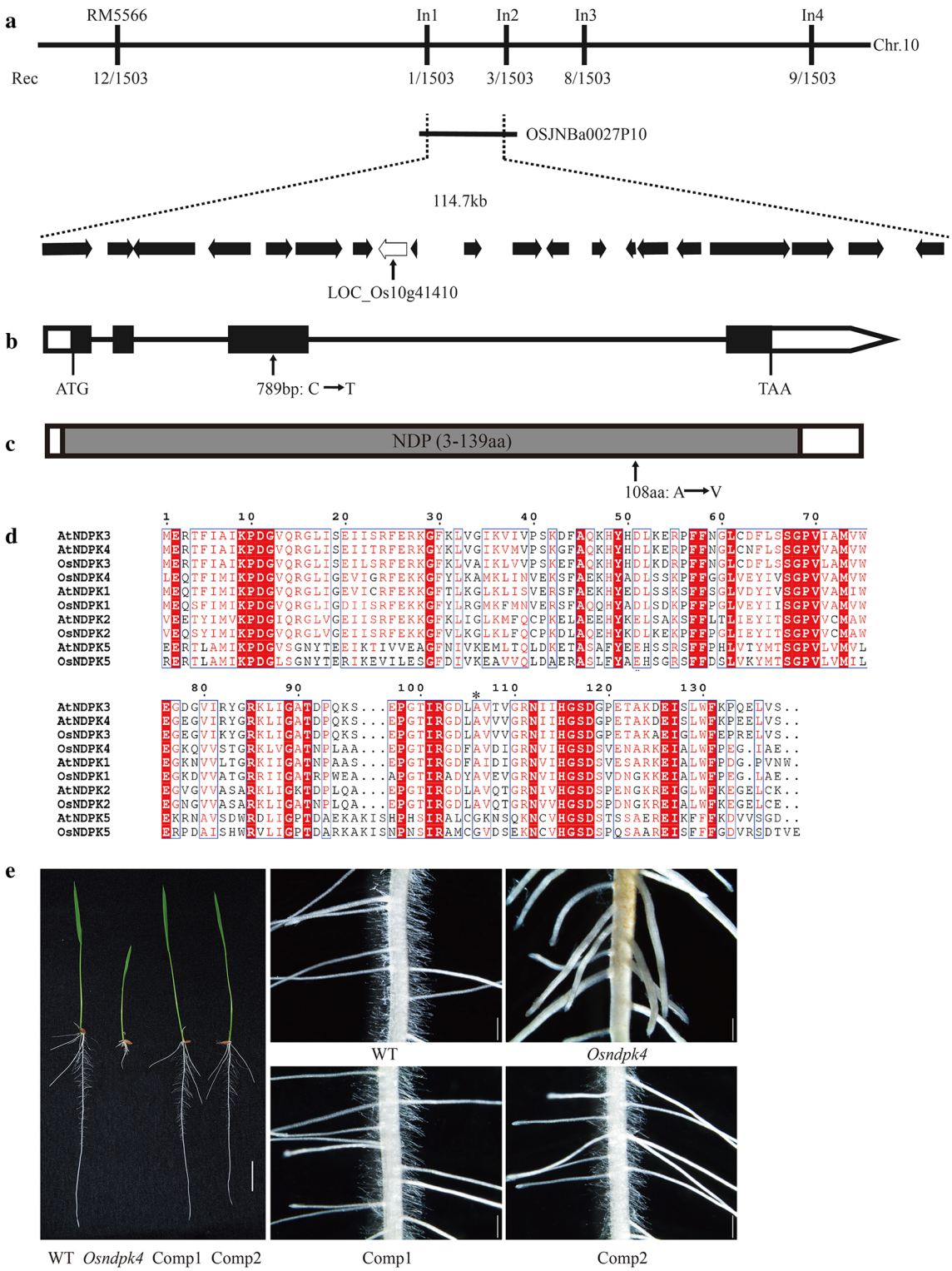

To further identify the biological pathways in which *OsNDPK4* may be involved, enrichment analysis of KEGG pathways for the DEGs between *Osndpk4* and WT was conducted. Thirty-two pathways were significantly enriched for up-regulated genes and nine for down-regulated ones (Supplementary Table S4). The top ten enriched pathways of the up-regulated DEGs were mainly related to carbonhydrate metabolism (galactose, amino sugar, and nucleotide sugar), lipid metabolism (fatty acid degradation, alpha-linolenic acid metabolism,

◂**Fig. 5** *OsNDPK4* encodes a NDPK protein in rice. **a** Map-based cloning of *OsNDPK4* within a 114.7 kb region on chromosome 10 between InDel markers In1 and In2. Twenty putative open reading frames were located in the 114.7 kb region. **b** The gene structure of *OsNDPK4*. Black boxes and lines represent exons and introns, respectively. White boxes indicate untranslated regions. The arrowhead shows the site of a single-base substitution (C to T) at the nucleotide 789 bp downstream of ATG. **c** Predicted domains of OsNDPK4 by the SMART database (https://smart.embl-heidelberg.de/). The arrowhead indicates the substitution within the NDP domain, which results in an amino acid substitution (Ala^{108} to Val^{108}). **d** Alignment of protein sequences of NDPKs from rice and *Arabidopsis*. The asterisk indicates the mutated residue in *Osndpk4*. **e** Complementation analysis of *Osndpk4*. The phenotype of O*sndpk4* was successfully recovered by transformation of *OsNDPK4* driven by its native promoter. Two independent lines of transgenic plants in the O*sndpk4* background were shown. Left, bar = 2 cm; right, bar = 500 μm

and peroxisome), amino acid metabolism (valine, leucine, and isoleucine degradation), secondary metabolism (biosynthesis of phenylpropanoid and diterpenoid), Plant-pathogen interaction and MAPK signaling pathway–plant, which was consistent with the putative role of OsNDPK4 in regulating energy homeostasis and the enhanced pathogen resistance observed in *Osndpk4* (Fig. 8c). The alpha-linolenic acid metabolism pathway is responsible for the synthesis of jasmonate, one of the major signaling molecules involved in plant root meristematic activity, and disease resistance (Chen et al. 2011; Nahar et al. 2011; Wasternack et al. 2013). The enriched pathways associated with down-regulated genes were mainly related to ribosome and ribosome biogenesis, DNA (purine and

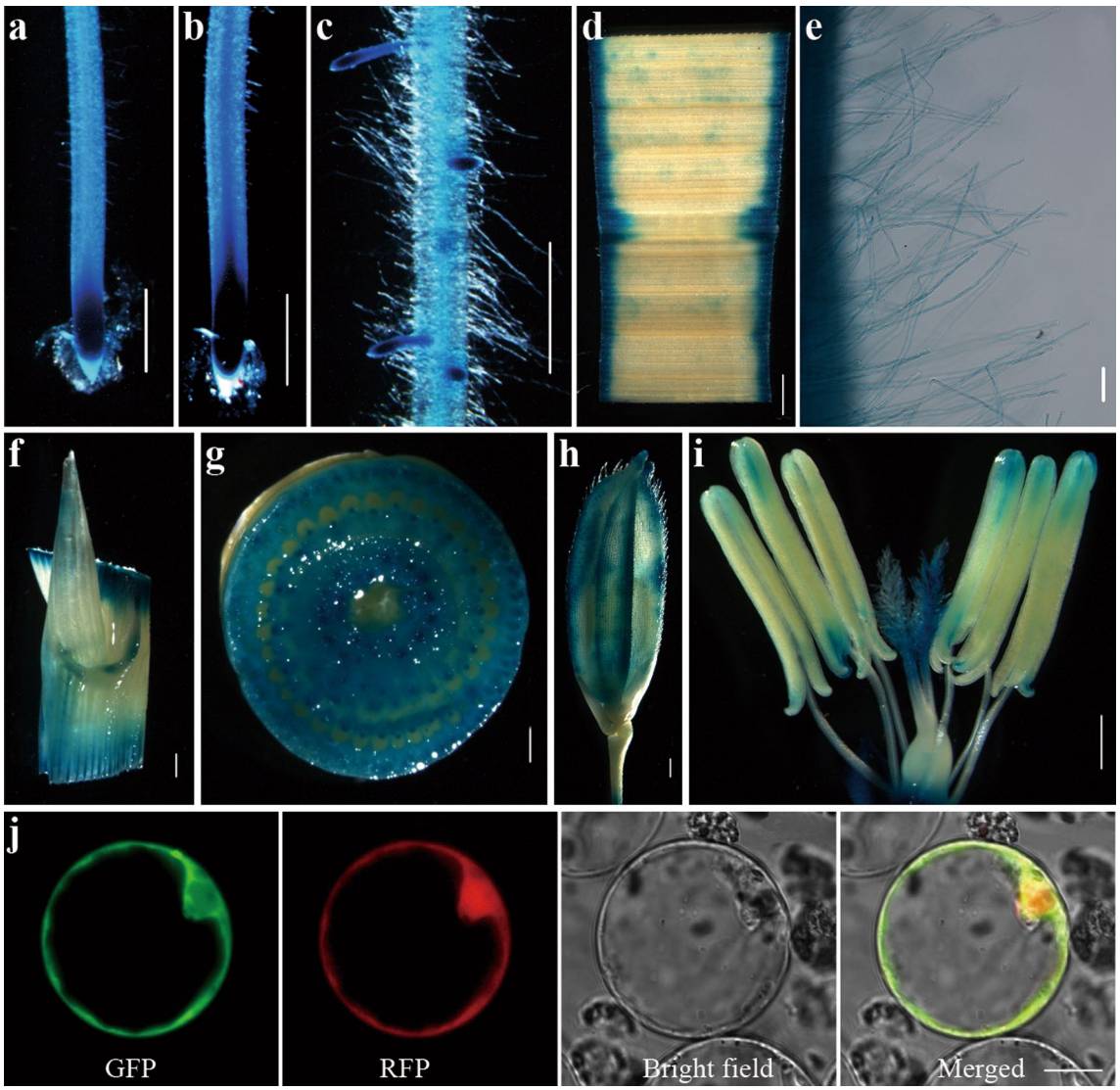

Fig. 6 Expression pattern of *OsNDPK4* and subcellular localization of OsNDPK4. **a**–**i** Histochemical staining analysis of expression of *OsNDPK4* promoter-GUS fusion in various tissues. GUS signals were detected in the primary root tip (**a**), adventitious root tip (**b**), tip and base of lateral roots (**c**), leaf (**d**), root hair (**e**), ligule (**f**), stem node (**g**), glume (**h**), pistils and stamen (**i**). Bars = 500 μm. **j** OsNDPK4 targets green fluorescent protein (GFP) to the cytosol in transiently transformed rice protoplasts cells. Bar = 10 μm

pyrimidine metabolism and DNA replication), photosynthesis (photosynthesis, antenna proteins, and carbon fixation), confirming the suppression of biosynthesis activities of carbohydrate, protein, and DNA in *Osndpk4* (Fig. 8d).

When examining the KEGG pathways in more detail, it was found that all steps of the fatty acid degradation pathway were highly up-regulated (Fig. 8e). It's known that during the early growth stage after germination, the carbohydrate and fatty acid storage in the seeds are supporting the growth of the young rice seedlings. Therefore, the higher expression of genes associated with fatty acid degradation in *Osndpk4* might be a result of slower consumption of energy storage due to retarded growth. Moreover, 230 ribosome proteins were found in DEGs, all but one of which was down-regulated (Supplementary Table S5). MapMan classification further confirmed that small and large subunits of ribosome for translation of nuclear genes, mitochondrial genes and chloroplast genes were all significantly down-regulated (Fig. 8f). In addition, 30 DEGs associated with ribosome biogenesis were found, among which 28 were also down-regulated (Supplementary Table S5). These results indicated significant reduction in protein translation in *Osndpk4* compared with WT.

Discussion

In the present study, a rice mutant *Osndpk4* was identified from an ethylmethane sulfonate-mutagenized population of rice (*indica*, Kasalath). The mutation caused loss-of-function of OsNDPK4, a nucleoside diphosphate kinase.

Fig. 8 Transcriptomic analysis of roots of 7-day-old *Osndpk4* by RNA-seq. Gene ontology (GO) enrichment of up- (**a**) and down-regulated (**b**) differentially expressed genes (DEGs) between WT and *Osndpk4*, respectively. KEGG pathway enrichment of up- (**c**) and down-regulated (**d**) DEGs between WT and *Osndpk4*. **e** Mapping of DEGs associated with the KEGG fatty acid degradation pathway. Boxes labelled with red color indicate up-regulated DEGs between WT and *Osndpk4*. **f** MapMan analysis of DEGs associated with ribosome proteins

The mutant showed severe defects in root system development, semi-dwarfness and reduced fertility (Figs. 1, 2, 3). Functional complementation with *OsNDPK4* rescued the mutant phenotype in *Osndpk4* (Fig. 5). Transcriptome analysis of *Osndpk4* and WT further revealed that DEGs were significantly associated with a number of biological processes, including metabolism, translation, biotic stress response, etc.

NDPKs belong to the Nme protein family involved in processes regulating cell proliferation of tumor metastases in animal (Roymans et al. 2002; Boissan et al. 2009). Transgenic study of OsNDPK1 in rice confirms the function of type I NDPK in plant growth and development (Pan et al. 2000). Knockdown of *OsNDPK1* resulted in growth defect, shorter mature plants, and reduced cell length in coleoptile epidermal cells, which suggests that *OsNDPK1* is involved in the cell elongation processes. Studies in potato have demonstrated remarkable differences in *NDPK1* expression among cell types, with predominant expression in meristematic zones and provascular tissues (Dorion et al. 2006). Manipulation of NDPK1 activity is also found to affect potato root growth (Dorion et al. 2017). Here, we identified *OsNDPK4*, another type

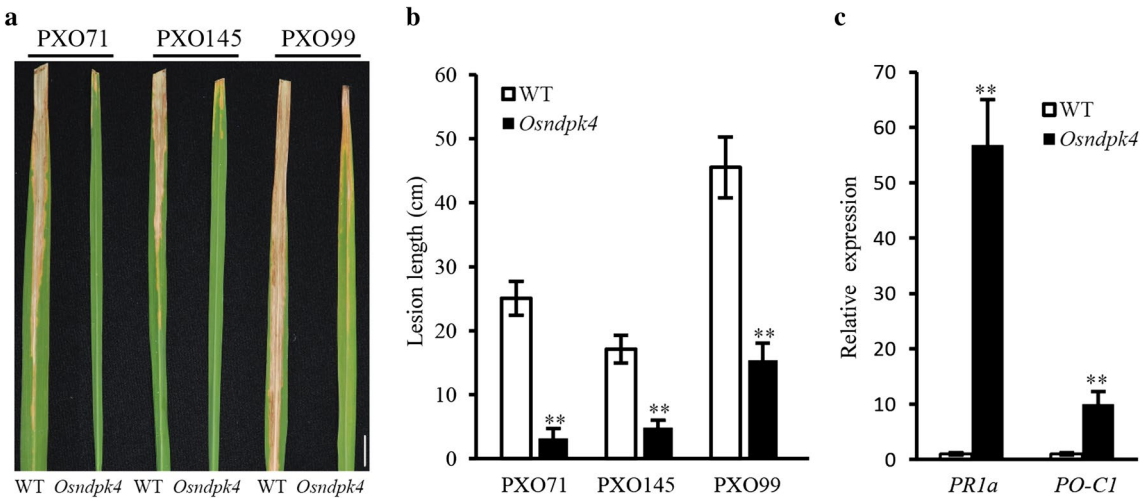

Fig. 7 Bacterial blight pathogen resistance and expression of resistance-related genes in *Osndpk4*. **a** Reactions of WT and *Osndpk4* to 3 *Xoo* isolates. Bar = 2 cm. **b** Lesion lengths of WT and *Osndpk4* to 3 *Xoo* isolates measured 3 weeks after infection. Data are means ± SD of ten plants. **c** Relative expression of pathogenesis-related genes in WT and *Osndpk4* leaves at the tillering stage. Data are means ± SD of three biological replicates (Student's *t* test: $^{**}P < 0.01$)

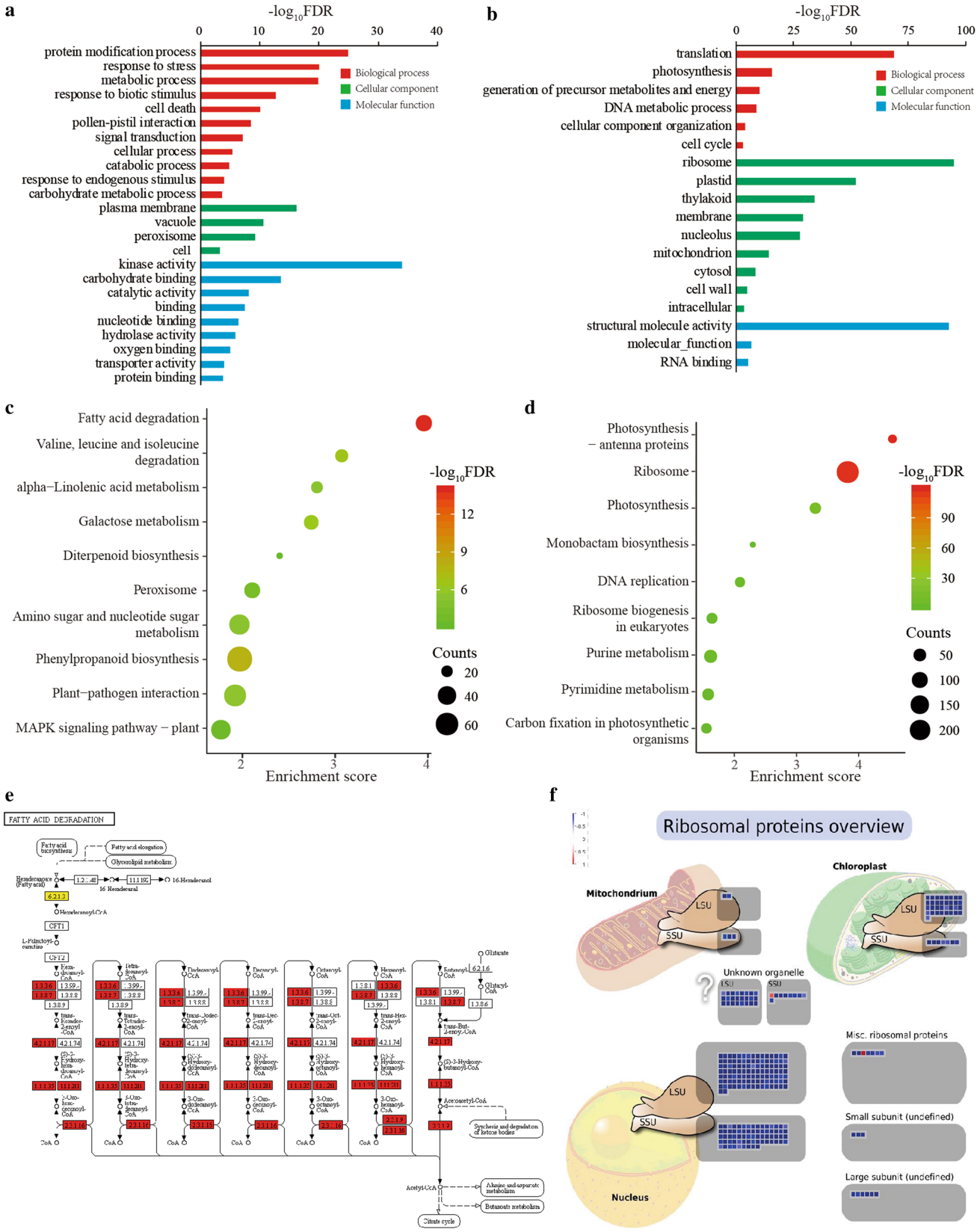
a
-log10FDR
0
10
20
30
40
protein modification process
response to stress
metabolic process
response to biotic stimulus
cell death
pollen-pistil interaction
signal transduction
cellular process
catabolic process
response to endogenous stimulus
carbohydrate metabolic process
plasma membrane
vacuole
peroxisome
cell
kinase activity
carbohydrate binding
catalytic activity
binding
nucleotide binding
hydrolase activity
oxygen binding
transporter activity
protein binding
Biological process
Cellular component
Molecular function
b
-log10FDR
0
25
50
75
100
translation
photosynthesis
generation of precursor metabolites and energy
DNA metabolic process
cellular component organization
cell cycle
ribosome
plastid
thylakoid
membrane
nucleolus
mitochondrion
cytosol
cell wall
intracellular
structural molecule activity
molecular_function
RNA binding
Biological process
Cellular component
Molecular function
c
Fatty acid degradation
Valine, leucine and isoleucine degradation
alpha−Linolenic acid metabolism
Galactose metabolism
Diterpenoid biosynthesis
Peroxisome
Amino sugar and nucleotide sugar metabolism
Phenylpropanoid biosynthesis
Plant−pathogen interaction
MAPK signaling pathway − plant
-log10FDR
12
9
6
Counts
20
40
60
2
3
4
Enrichment score
d
Photosynthesis − antenna proteins
Ribosome
Photosynthesis
Monobactam biosynthesis
DNA replication
Ribosome biogenesis in eukaryotes
Purine metabolism
Pyrimidine metabolism
Carbon fixation in photosynthetic organisms
-log10FDR
90
60
30
Counts
50
100
150
200
2
3
4
Enrichment score
e
FATTY ACID DEGRADATION
f
Ribosomal proteins overview
Mitochondrium
LSU
SSU
Chloroplast
LSU
SSU
Unknown organelle
LSU
SSU
LSU
SSU
Nucleus
Misc. ribosomal proteins
Small subunit (undefined)
Large subunit (undefined)

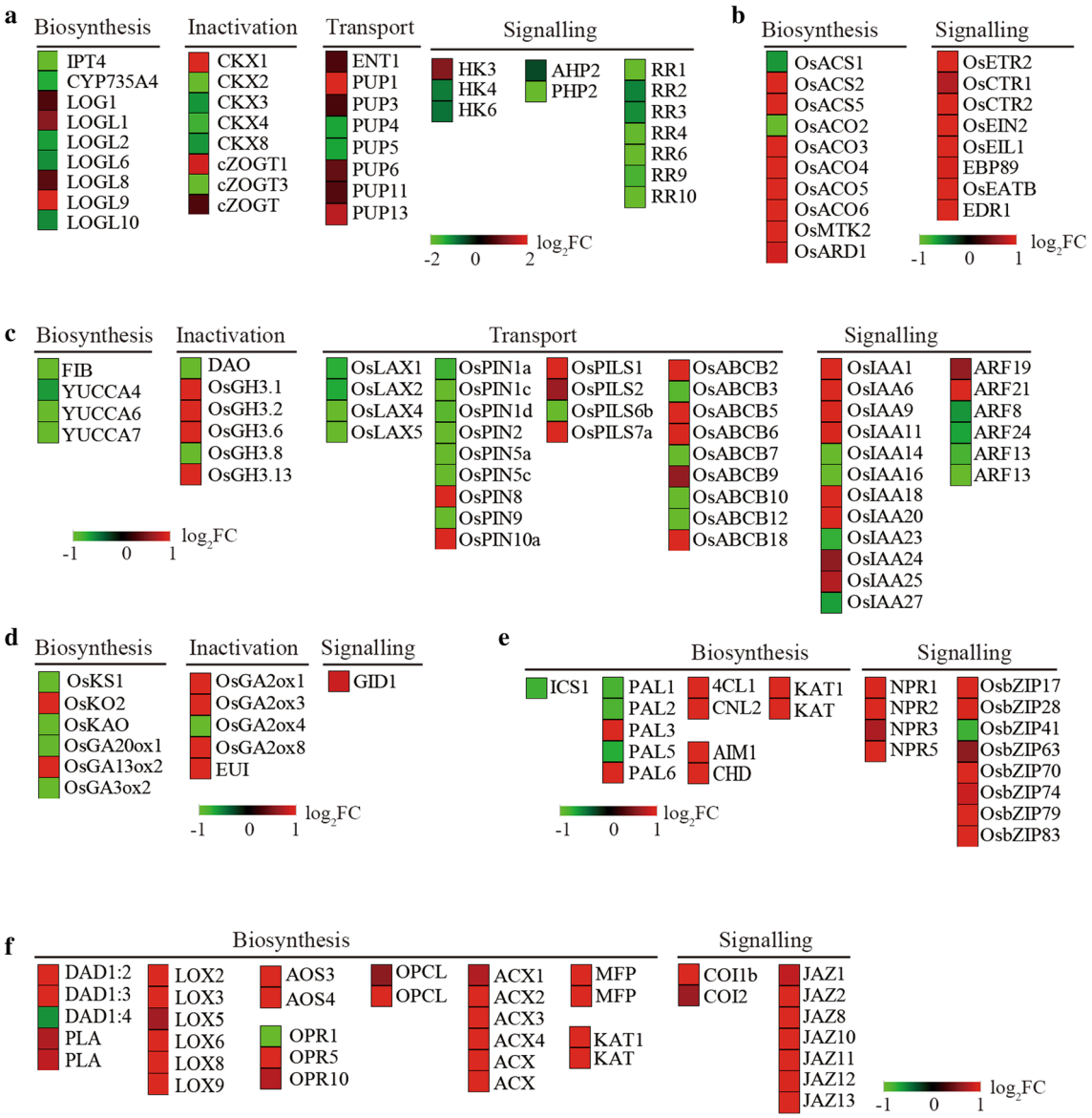

Fig. 9 Expression profiles of DEGs associated with metabolism, transport, and signalling of hormones. **a** Heat map of DEGs involved in biosynthesis, inactivation, transport, and signalling of cytokinin. **b** Heat map of DEGs involved in biosynthesis and signalling of ethylene. **c** Heat map of DEGs involved in biosynthesis, inactivation, transport, and signalling of auxin. **d** Heat map of DEGs involved in biosynthesis, inactivation and signalling of gibberellin. **e** Heat map of DEGs involved in biosynthesis and signalling of SA. **f** Heat map of DEGs involved in biosynthesis and signalling of jasmonate. Color scale represents log2 (fold change of gene expression between *Osndpk4* and WT)

I NDPK in rice, and found that OsNDPK4 is critical for maintaining root meristem activity and cell elongation (Fig. 2a–f), which is further evidenced by the high expression in tip regions of primary roots, adventitious roots, and lateral roots (Fig. 6a–c). ROS regulates the balance between cellular proliferation and differentiation in roots (Tsukagoshi et al. 2010). The reduced ROS level observed in the root of *Osndpk4* indicates that OsNDPK4 is critical for maintaining ROS levels in root tips (Fig. 4b, c).

Besides a crucial role in NTP metabolism, plant NDPK isoforms play roles in different processes based on their subcellular localization. NDPK isoforms in plants have been shown to be located in various subcellular compartments (Sweetlove et al. 2001; Cho et al. 2004; Dorion and Rivoal 2015). Type I NDPKs are believed to be located in the cytosol due to lack of targeting sequences (Dorion et al. 2006), types II and III NDPKs have N terminal extensions and are thought to be located in the chloroplast

and/or mitochondria (Sweetlove et al. 2001), while type IV NDPKs putatively localize in the ER (Dorion and Rivoal 2015). The predicted subcellular localization of type I NDPKs in the cytosol is supported by experimental studies using transient expression of AtNDPK1 and OsNDPK1 fused to fluorescent proteins (Reumann et al. 2009; Kihara et al. 2011). Here, we found that OsNDPK4 located in the cytosol (Fig. 5j), which is consistent with a previous prediction (Cho et al. 2004). The same subcellular localization of OsNDPK4 and OsNDPK1 is consistent with their putative functional redundancy, which could facilitate one to effectively compensate the functional loss of the other. However, the severe phenotype observed in *Osndpk4* shows that NDPK1 is not sufficient to complement the NDPK4 deficiency. This suggests functional specificity between NDPK1 and NDPK4. Moreover, eukaryotic NDPKs could form homo- and/or heterohexamers (Johansson et al. 2004). The aberrant NDPK4 in *Osndpk4* might disturb NDPK activities in the cytosol by formation of functionally impaired NDPK1–NDPK4 heterohexamers.

It's known that hormone crosstalk plays critical roles in growth and defense trade-offs of plants (Berens et al. 2017). Among them, auxin and cytokinins are two classic hormones regulating growth, jasmonate and SA are major positive regulators of plant defense, while ethylene and gibberellins are important modulators of both growth and defense. Analysis of DEGs in *Osndpk4* found that a number of genes encoding key members were associated with these hormones ranging from metabolism, transport to signalling (Fig. 9a–f). It was seen that the cytokinin signalling pathway was repressed in *Osndpk4* (Fig. 9a), which is consistent with the observed reduced root meristem activity. Corresponding with it, 19 key regulatory components of the cell cycle were found in DEGs and 17 of them were down-regulated, including 2 CDKs, 11 cyclins, 2 RBs, CKS1, DEL2, E2F2, and KRP5 (Supplementary Table S6), suggesting repression of cell division in *Osndpk4*. The biosynthesis and signalling of ethylene were significantly enhanced (Fig. 9b), which is consistent with previous reports of its inhibition of rice root development (Růžička et al. 2007; Yang et al. 2015). An auxin gradient is critical for cell division and cell elongation as shown by retarded root growth of *PIN* mutants in *Arabidopsis* (Blilou et al. 2005). A broad down- and up-regulation of its transport components were observed (Fig. 9c), including 4 out of total 5 *AUX/LAX*s and 9 out of total 12 *PINs* in the rice genome, which indicates disturbance of the auxin gradient along the root of *Osndpk4*. Gibberellins are believed to promote root cell elongation in the elongation zone (Takatsuka and Umeda 2014). In line with it, repression of gene encoding key enzymes for biosynthesis and induction of genes encoding deactivating enzymes for gibberellins were observed in *Osndpk4* (Fig. 9d). The biosynthesis and signalling of SA and jasmonate were both significantly activated in *Osndpk4* (Fig. 9e, f), which might lead to the retarded root growth and enhanced resistance against bacterial blight (Fig. 7a, b) (Chen et al. 2011; Xu et al. 2017).

Enhanced expression of *OsNDPK1* in rice was observed upon infection with bacterial pathogens (Cho et al. 2004). In the present study, we showed that the loss-of-function of OsNDPK4 resulted in enhanced resistances to rice bacterial blight (Fig. 7a, b). The accumulation of pathogenesis-related (PR) proteins is one of the most-characterized plant-defense responses. The expression of two PR marker genes, *PR1b* and *PO-C1*, was both significantly up-regulated in *Osndpk4* (Fig. 6c), indicating activation of PR genes and their possible roles in the enhanced pathogen resistance. Whole-genome transcriptome analysis displayed that there were 50 previously reported PRs in the DEGs and all but two of them were significantly up-regulated in *Osndpk4* (Supplementary Table S7). Moreover, WRKY transcription factors are key components in SA-dependent defense responses regulating PR gene expression (Jimmy and Babu 2015). In our study, there were 55 WRKY genes showing differential expression in *Osndpk4* compared with the WT, and 52 of them were up-regulated (Supplementary Table S8).

In conclusion, we report herein that *OsNDPK4* regulates development-defense trade-offs in rice. We characterized the roles of this rice protein, and revealed that loss-of-function of *OsNDPK4* resulted in defective root development and elevated pathogen resistance.

Author contribution statement WD, BZ, and SZ conceived and designed the experiments. JY, WD, YC, XZ, JS, and WZ performed the experiments. WD, BZ, and SZ analysed the data and wrote the paper. All authors read and approved the final manuscript.

Acknowledgements This work was supported by the National Natural Science Foundation of China [Grant Numbers 31300246, 31371595], the Zhejiang Provincial Natural Science Foundation of China [Grant Numbers LY17C020002], the Natural Science Foundation of Ningbo [Grant Number 2019A610413] and K. C. Wong Magna Fund in Ningbo University.

Compliance with ethical standards

Conflict of interest The authors have no conflict of interest to declare.

References

Ahsan N, Lee DG, Lee KW, Alam I, Lee SH, Bahk JD, Lee BH (2008) Glyphosate-induced oxidative stress in rice leaves revealed by proteomic approach. Plant Physiol Biochem 46(12):1062–1070

Anders S, Pyl PT, Huber W (2015) HTSeq—a python framework to work with high-throughput sequencing data. Bioinformatics 31(2):166–169

Berens ML, Berry HM, Mine A, Argueso CT, Tsuda K (2017) Evolution of hormone signaling networks in plant defense. Annu Rev Phytopathol 55(1):401–425

Blilou I, Xu J, Wildwater M, Willemsen V, Paponov I, Friml J, Heidstra R, Aida M, Palme K, Scheres B (2005) The PIN auxin efflux facilitator network controls growth and patterning in *Arabidopsis* roots. Nature 433:39–44

Boissan M, Dabernat S, Peuchant E, Schlattner U, Lascu I, Lacombe M-L (2009) The mammalian Nm23/NDPK family: from metastasis control to cilia movement. Mol Cell Biochem 329(1):51–62

Carol RJ, Takeda S, Linstead P, Durrant MC, Kakesova H, Derbyshire P, Drea S, Zarsky V, Dolan L (2005) A RhoGDP dissociation inhibitor spatially regulates growth in root hair cells. Nature 438(7070):1013–1016

Chen S, Jin W, Wang M, Zhang F, Zhou J, Jia Q, Wu Y, Liu F, Wu P (2003) Distribution and characterization of over 1000 T-DNA tags in rice genome. Plant J 36(1):105–113

Chen Q, Sun J, Zhai Q, Zhou W, Qi L, Xu L, Wang B, Chen R, Jiang H, Qi J, Li X, Palme K, Li C (2011) The basic helix-loop-helix transcription factor MYC2 directly represses *PLETHORA* expression during jasmonate-mediated modulation of the root stem cell niche in *Arabidopsis*. Plant Cell 23(9):3335–3352

Chen J, Lin T, Xu H, Tian D, Luo Y, Ren C, Yang L, Shi J (2012) Cold-induced changes of protein and phosphoprotein expression patterns from rice roots as revealed by multiplex proteomic analysis. Plant Omics 5(2):194–199

Cho SM, Shin SH, Kim KS, Kim YC, Eun MY, Cho BH (2004) Enhanced expression of a gene encoding a nucleoside diphosphate kinase 1 (OsNDPK1) in rice plants upon infection with bacterial pathogens. Mol Cells 18(3):390–395

Choi G, Kim J-I, Hong S-W, Shin B, Choi G, Blakeslee JJ, Murphy AS, Seo YW, Kim K, Koh E-J, Song P-S, Lee H (2005) A possible role for NDPK2 in the regulation of auxin-mediated responses for plant growth and development. Plant Cell Physiol 46(8):1246–1254

Ding WN, Lin L, Zhang BT, Xiang XB, Wu J, Pan ZC, Zhu SH (2015) OsKASI, a β-ketoacyl-[acyl carrier protein] synthase I, is involved in root development in rice (*Oryza sativa* L.). Planta 242(1): 203–213

Ding W, Wu J, Ye J, Zheng W, Wang S, Zhu X, Zhou J, Pan Z, Zhang B, Zhu S (2018) A *Pelota-like* gene regulates root development and defence responses in rice. Ann Bot 122(3):359–371

Dorion S, Rivoal J (2015) Clues to the functions of plant NDPK isoforms. Naunyn-Schmiedeberg's Arch Pharmacol 388(2):119–132

Dorion S, Matton DP, Rivoal J (2006) Characterization of a cytosolic nucleoside diphosphate kinase associated with cell division and growth in potato. Planta 224(1):108–124

Dorion S, Clendenning A, Rivoal J (2017) Engineering the expression level of cytosolic nucleoside diphosphate kinase in transgenic solanum tuberosum roots alters growth, respiration and carbon metabolism. Plant J 89(5):914–926

Edlund B (1971) Purification of a nucleoside diphosphate kinase from pea seed and phosphorylation of the enzyme with adenosine (32 p) triphosphate. Acta Chem Scand 25(4):1370–1376

Fatehi F, Hosseinzadeh A, Alizadeh H, Brimavandi T (2013) The proteome response of *Hordeum spontaneum* to salinity stress. Cereal Res Commun 41(1):78–87

Feng BH, Yang Y, Shi YF, Shen HC, Wang HM, Huang QN, Xu X, Lu XG, Wu JL (2013) Characterization and genetic analysis of a novel rice spotted-leaf mutant HM47 with broad-spectrum resistance to *Xanthomonasoryzae* pv. *oryzae*. J Integr Plant Biol 55(5):473–483

Fukamatsu Y, Yabe N, Hasunuma K (2003) *Arabidopsis* NDK1 is a component of ROS signaling by interacting with three catalases. Plant Cell Physiol 44(10):982–989

Gaff DF, Okong'O-Ogola O (1971) The use of non-permeating pigments for testing the survival of cells. J Exp Bot 22(3):756–758

Hammargren J, Rosenquist S, Jansson C, Knorpp C (2008) A novel connection between nucleotide and carbohydrate metabolism in mitochondria: sugar regulation of the *Arabidopsis* nucleoside diphosphate kinase 3a gene. Plant Cell Rep 27(3):529–534

Haque ME, Yoshida Y, Hasunuma K (2010) ROS resistance in *Pisum-sativum* cv. *Alaska*: the involvement of nucleoside diphosphate kinase in oxidative stress responses via the regulation of antioxidants. Planta 232(2):367–382

Harris N, Taylor JE, Roberts JA (1994) Isolation of a mRNA encoding a nucleoside diphosphate kinase from tomato that is up-regulated by wounding. Plant Mol Biol 25(4):739–742

Hetmann A, Kowalczyk S (2009) Nucleoside diphosphate kinase isoforms regulated by phytochrome A isolated from oat coleoptiles. Acta Biochim Pol 56(1):143–153

Jimmy JL, Babu S (2015) Role of OsWRKY transcription factors in rice disease resistance. Trop Plant Pathol 40(6):355–361

Johansson M, MacKenzie-Hose A, Andersson I, Knorpp C (2004) Structure and mutational analysis of a plant mitochondrial nucleoside diphosphate kinase. Identification of residues involved in serine phosphorylation and oligomerization. Plant Physiol 136(2):3034–3042

Kano A, Gomi K, Yamasaki-Kokudo Y, Satoh M, Fukumoto T, Ohtani K, Tajima S, Izumori K, Tanaka K, Ishida Y, Tada Y, Nishizawa Y, Akimitsu K (2010) A rare sugar, D-allose, confers resistance to rice bacterial blight with upregulation of defense-related genes in *Oryza sativa*. Phytopathology 100(1):85–90

Kauffman HE, Reddy APK, Hsieh SPY, Merca SD (1973) An improved technique for evaluating resistance of rice varieties to *Xanthomonas oryzae*. Plant Dis Rep 57:537–541

Kawasaki S, Borchert C, Deyholos M, Wang H, Brazille S, Kawai K, Galbraith D, Bohnert HJ (2001) Gene expression profiles during the initial phase of salt stress in rice. Plant Cell 13(4):889–905

Kihara A, Saburi W, Wakuta S, Kim M-H, Hamada S, Ito H, Imai R, Matsui H (2011) Physiological and biochemical characterization of three nucleoside diphosphate kinase isozymes from rice (*Oryzasativa* L.). Biosci Biotech Biochem 75(9):1740–1745

Lee D-G, Ahsan N, Lee S-H, Kang KY, Lee JJ, Lee B-H (2007) An approach to identify cold-induced low-abundant proteins in rice leaf. CR Biol 330(3):215–225

Lin S-K, Chang M-C, Tsai Y-G, Lur H-S (2005) Proteomic analysis of the expression of proteins related to rice quality during caryopsis development and the effect of high temperature on expression. Proteomics 5(8):2140–2156

Love MI, Huber W, Anders S (2014) Moderated estimation of fold change and dispersion for RNA-seq data with DESeq2. Genome Biol 15(12):550

Mehta A, Orchard S (2009) Nucleoside diphosphate kinase (NDPK, NM23, AWD): recent regulatory advances in endocytosis, metastasis, psoriasis, insulin release, fetal erythroid lineage and heart failure; translational medicine exemplified. Mol Cell Biochem 329(1):3–15

Miao Y, Jiang L (2007) Transient expression of fluorescent fusion proteins in protoplasts of suspension cultured cells. Nat Protoc 2(10):2348–2353

Moon H, Lee B, Choi G, Shin D, Prasad DT, Lee O, Kwak SS, Kim DH, Nam J, Bahk J, Hong JC, Lee SY, Cho MJ, Lim CO, Yun DJ (2003) NDP kinase 2 interacts with two oxidative stress-activated MAPKs to regulate cellular redox state and enhances multiple stress tolerance in transgenic plants. Proc Natl Acad Sci USA 100(1):358–363

Nahar K, Kyndt T, De Vleesschauwer D, Höfte M, Gheysen G (2011) The jasmonate pathway is a key player in systemically induced defense against root knot nematodes in rice. Plant Physiol 157(1):305–316

Nomura T, Yatsunami K, Honda A, Sugimoto Y, Fukui T, Zhang J, Yamamoto J, Ichikawa A (1992) The amino acid sequence of nucleoside diphosphate kinase i from spinach leaves, as deduced from the cDNA sequence. Arch Biochem Biophys 297(1):42–45

Pan L, Kawai M, Yano A, Uchimiya H (2000) Nucleoside diphosphate kinase required for coleoptile elongation in rice. Plant Physiol 122(2):447–452

Parks RE, Aganwal RP (1973) 9 nucleoside diphosphokinases. In: Boyer PD (ed) The enzymes, 8th edn. Academic Press, Cambridge, pp 307–333

Reumann S, Quan S, Aung K, Yang P, Manandhar-Shrestha K, Holbrook D, Linka N, Switzenberg R, Wilkerson CG, Weber APM, Olsen LJ, Hu J (2009) In-depth proteome analysis of *Arabidopsis* leaf peroxisomes combined with in vivo subcellular targeting verification indicates novel metabolic and regulatory functions of peroxisomes. Plant Physiol 150(1):125–143

Roymans D, Willems R, Van Blockstaele DR, Slegers H (2002) Nucleoside diphosphate kinase (NDPK/NM23) and the waltz with multiple partners: possible consequences in tumor metastasis. Clin Exp Metastasis 19(6):465–476

Růžička K, Ljung K, Vanneste S, Podhorská R, Beeckman T, Friml J, Benková E (2007) Ethylene regulates root growth through effects on auxin biosynthesis and transport-dependent auxin distribution. Plant Cell 19(7):2197–2212

Salekdeh GH, Siopongco J, Wade LJ, Ghareyazie B, Bennett J (2002) Proteomic analysis of rice leaves during drought stress and recovery. Proteomics 2(9):1131–1145

Sweetlove LJ, Mowday B, Hebestreit HF, Leaver CJ, Millar AH (2001) Nucleoside diphosphate kinase III is localized to the inter-membrane space in plant mitochondria. FEBS Lett 508(2):272–276

Takatsuka H, Umeda M (2014) Hormonal control of cell division and elongation along differentiation trajectories in roots. J Exp Bot 65(10):2633–2643

Thimm O, Bläsing O, Gibon Y, Nagel A, Meyer S, Krüger P, Selbig J, Müller LA, Rhee SY, Stitt M (2004) MapMan: a user-driven tool to display genomics data sets onto diagrams of metabolic pathways and other biological processes. Plant J 37(6):914–939

Trapnell C, Roberts A, Goff L, Pertea G, Kim D, Kelley DR, Pimentel H, Salzberg SL, Rinn JL, Pachter L (2012) Differential gene and transcript expression analysis of RNA-seq experiments with TopHat and Cufflinks. Nat Protoc 7(3):562–578

Tsukagoshi H, Busch W, Benfey PN (2010) Transcriptional regulation of ROS controls transition from proliferation to differentiation in the root. Cell 143(4):606–616

Veljovic-Jovanovic S, Noctor G, Foyer CH (2002) Are leaf hydrogen peroxide concentrations commonly overestimated? The potential influence of artefactual interference by tissue phenolics and ascorbate. Plant Physiol Biochem 40(6):501–507

Verslues PE, Kim Y-S, Zhu J-K (2007) Altered ABA, proline and hydrogen peroxide in an *Arabidopsis* glutamate:glyoxylate aminotransferase mutant. Plant Mol Biol 64(1):205–217

Wasternack C, Hause B (2013) Jasmonates: BIOSYNTHESIS, perception, signal transduction and action in plant stress response, growth and development. An update to the 2007 review in annals of botany. Ann Bot 111:1021–1058

Xu L, Zhao H, Ruan W, Deng M, Wang F, Peng J, Luo J, Chen Z, Yi K (2017) ABNORMAL INFLORESCENCE MERISTEM1 functions in salicylic acid biosynthesis to maintain proper reactive oxygen species levels for root meristem activity in rice. Plant Cell 29:560–574

Yang C, Lu X, Ma B, Chen S-Y, Zhang J-S (2015) Ethylene signaling in rice and *Arabidopsis*: conserved and diverged aspects. Mol Plant 8(4):495–505

Yano A, Shimazaki T, Kato A, Umeda M, Uchimiya H (1993) Molecular cloning and nucleotide sequence cDNA encoding nucleoside diphosphate kinase of rice (*Oryza sativa* L.). Plant Mol Biol 23:1087–1090

Ye W, Hu S, Wu L, Ge C, Cui Y, Chen P, Wang X, Xu J, Ren D, Dong G, Qian Q, Guo L (2016) White stripe leaf 12 (*WSL12*), encoding a nucleoside diphosphate kinase 2 (OsNDPK2), regulates chloroplast development and abiotic stress response in rice (*Oryzasativa* L.). Mol Breed 36(5):57

Zhang J, Movahedi A, Sang M, Wei Z, Xu J, Wang X, Wu X, Wang M, Yin T, Zhuge Q (2017) Functional analyses of NDPK2 in *Populus trichocarpa* and overexpression of *PtNDPK2* enhances growth and tolerance to abiotic stresses in transgenic poplar. Plant Physiol Biochem 117:61–74

Zhu Z-X, Liu Y, Liu S-J, Mao C-Z, Wu Y-R, Wu P (2012) A gain-of-function mutation in *OsIAA11* affects lateral root development in rice. Mol Plant 5(1):154–161

Affiliations

Jin Ye[1,2] · Wona Ding[1] · Yujie Chen[1] · Xinni Zhu[1] · Jiutong Sun[1] · Wenjuan Zheng[1] · Botao Zhang[3] · Shihua Zhu[1]

[1] College of Science and Technology, Ningbo University, Ningbo 315211, People's Republic of China

[2] School of Marine Sciences, Ningbo University, Ningbo 315211, People's Republic of China

[3] Cixi Institute of Biomedical Engineering, Ningbo Institute of Materials Technology and Engineering, Chinese Academy of Sciences, Ningbo 315201, China